Nuclear Physics B305 [FS23] (1988) 143–153
North-Holland, Amsterdam

PERCOLATION CLUSTER ALGORITHM AND SCALING BEHAVIOUR IN THE 4-DIMENSIONAL ISING MODEL

I. MONTVAY

Deutsches Elektronen-Synchrotron DESY, D-2000 Hamburg, FRG

G. MÜNSTER

II. Institut für Theoretische Physik der Universität Hamburg, D-2000 Hamburg, FRG

U. WOLFF

Institut für Theoretische Physik der Universität Kiel, D-2300 Kiel, FRG

Received 25 April 1988
(Revised 2 June 1988)

The scaling behaviour of renormalized quantities and the validity of renormalized perturbation theory is tested numerically in the symmetric phase of the 4-dimensional Ising model. The high-precision Monte Carlo calculation is based on an efficient percolation cluster algorithm.

1. Introduction

The Ising model is the limit of a single-component ϕ^4 theory at infinite bare quartic self-coupling (λ). A lot is known about the ϕ^4 model in four dimensions. In the continuum limit the renormalized coupling (g_R) is most probably zero, independently of the value of the bare self-coupling ("triviality") [1]. Correspondingly, there is a cut-off-dependent upper limit on the renormalized coupling which vanishes logarithmically with the cut-off. The largest possible value of g_R is probably reached in the Ising limit. The behaviour of renormalized quantities, for large cut-off in the scaling region near the critical line, is controlled by the Callan–Symanzik renormalization group equations [2]. Assuming this general behaviour, it is possible to give an approximate analytical solution of the ϕ^4 model everywhere in the physically interesting scaling region [3, 4] by starting from a high-order hopping parameter expansion ("high-temperature expansion") and using it as an initial condition for the integration of the Callan–Symanzik equations. The success of this procedure relies on the fact that in the whole scaling region the renormalized coupling is small enough for the application of renormalized perturbation theory.

0169-6823/88/$03.50

The solution of the renormalization group equations can also be continued over the critical theory into the phase with spontaneously broken symmetry [3]. This is where the study of simple ϕ^4 models has its physical motivation, because the prototype model of the Higgs sector of the standard electroweak theory is a (four-component) ϕ^4 model with spontaneously broken symmetry. In this context, due to the triviality of the continuum limit, one has to assume that in the Higgs sector, for some physical reason, the cut-off is finite. This allows for a non-zero renormalized quartic interaction of the scalar field. On the lattice the physical cut-off is replaced by the inverse lattice spacing, but in the scaling region, where the cut-off is much larger than the physical mass scale, this replacement is legitimate because the cut-off effects on physical quantities are negligible.

For the study of lattice ϕ^4 models, high-precision numerical Monte Carlo calculations are particularly useful on the edges of the scaling region, in order to check the general consistency of the analytical approach and to control the error estimates. Precise numerical calculations are feasible in the region with correlation lengths of the order of 1–10. This is just the region where both components of the analytical calculation (hopping parameter expansion and renormalized perturbation theory) are driven to the limits of their validity in order to join them together. From this point of view the calculations in the limit of infinite bare coupling are most useful, because the analytical approximations are poorest in this case. It is a fortunate circumstance that the numerical Monte Carlo calculations are particularly easy just in this limit, because one can use specific techniques applicable to Ising models. A highly efficient method of simulating Ising-like systems was developed recently by Swendsen and Wang [5]. It is based on the mapping of the Ising spin model onto a percolation cluster model [6]. As it was shown in ref. [5], critical slowing down is drastically reduced in two and three dimensions by this algorithm.

In this paper the results of a high-precision numerical Monte Carlo simulation of the 4-dimensional Ising model, based on the percolation cluster algorithm, are presented. Our aim is to check in the symmetric phase the validity of renormalized perturbation theory and, in particular, of the perturbative scaling for renormalized quantities. The precise numerical data can also be taken as initial conditions for the integration of the renormalization group equations. This implies smaller errors for the predictions on the broken-symmetry side of the critical point. As a by-product, the merits and drawbacks of the percolation cluster algorithm are experienced in a large-scale 4-dimensional computation. For comparison, and as a basis for choosing the parameters of the calculation, we shall use the results of a recent study of the finite-volume effects in the 4-dimensional Ising model [7].

As described in ref. [5], the Monte Carlo simulation in the percolation cluster algorithm proceeds by generating an alternating sequence of spin- and bond-configurations. The bond configuration is represented by the values 0 or 1 on the links which connect neighbouring lattice sites. A cluster is a maximal set of points connected by bonds with value 1. The efficiency of the cluster updating algorithm in

fighting critical slowing-down is due to the fact that in the step from the bond-configuration to the spin-configuration whole clusters are statistically assigned a new spin value. Since there are also large clusters, this can imply a non-local change of spins. There is, however, also another advantage of the algorithm which turned out to be even more important in our calculations with moderate correlation lengths in four dimensions. Namely, the generated sequence of bond-configurations and their cluster structure can also be used to measure physical quantities. In this way one obtains the same expectation values as in the spin representation, but the fluctuations, and therefore the statistical errors, are smaller [8]. In fact, it turned out in our calculations that in many cases the cluster representation is a highly efficient variance-reduction method [9, 10].

2. Presentation and discussion of the results

The cluster representation of simple quantities is easily obtained from the definitions [5], therefore we give here only a few examples and leave the derivation to the interested reader. The expectation value of the product of two spins (with $\sigma_x = \pm 1$) is given in the cluster language by

$$\langle \sigma_x \sigma_y \rangle = \langle C_{xy} \rangle', \tag{1}$$

where the prime denotes an expectation value on the sequence of bond-configurations, and the function C_{xy} is defined to be 1 if the points x, y belong to the same cluster and 0 otherwise. The cluster representation of the susceptibility χ_2 is, accordingly

$$\chi_2 \equiv \frac{1}{N} \sum_{xy} \langle \sigma_x \sigma_y \rangle = \frac{1}{N} \left\langle \sum_c n_c^2 \right\rangle' . \tag{2}$$

Here N is the number of lattice points, Σ_c means a summation over the clusters and n_c denotes the number of points in the cluster c. Note that in a cluster simulation the sign of the total spin always fluctuates such that its average vanishes at any hopping parameter κ. This is different for local algorithms, as e.g. the Metropolis algorithm [11], where in the broken phase the metastability of a given sign of the average spin can persist for a very long time. This implies that the definition of the connected quantities in the phase with broken symmetry requires some care. (For a detailed study of the broken phase of the 4-dimensional Ising model with the help of the percolation cluster algorithm see ref. [12].) Returning to the cluster representation of some important physical quantities, the formulae for the higher susceptibili-

ties χ_4 and χ_6 (sums of the connected 4-, respectively, 6-point functions) are

$$\chi_4 \equiv \frac{1}{N} \sum_{x_1, x_2, x_3, x_4} \langle \sigma_{x_1} \sigma_{x_2} \sigma_{x_3} \sigma_{x_4} \rangle_c$$

$$= -\frac{2}{N} \left\langle \sum_c n_c^4 \right\rangle' + \frac{3}{N} \left[\left\langle \sum_{c_1 c_2} n_{c_1}^2 n_{c_2}^2 \right\rangle' - \left\langle \sum_c n_c^2 \right\rangle'^2 \right], \tag{3}$$

$$\chi_6 \equiv \frac{1}{N} \sum_{x_1, \ldots, x_6} \langle \sigma_{x_1}, \ldots, \sigma_{x_6} \rangle_c$$

$$= \frac{16}{N} \left\langle \sum_c n_c^6 \right\rangle' - \frac{30}{N} \left[\left\langle \sum_{c_1 c_2} n_{c_1}^4 n_{c_2}^2 \right\rangle' - \left\langle \sum_{c_1} n_{c_1}^4 \right\rangle' \left\langle \sum_{c_2} n_{c_2}^2 \right\rangle' \right]$$

$$+ \frac{15}{N} \left[\left\langle \sum_{c_1 c_2 c_3} n_{c_1}^2 n_{c_2}^2 n_{c_3}^2 \right\rangle' - 3 \left\langle \sum_{c_1 c_2} n_{c_1}^2 n_{c_2}^2 \right\rangle' \left\langle \sum_{c_3} n_{c_3}^2 \right\rangle' + 2 \left\langle \sum_c n_c^2 \right\rangle'^3 \right]. \tag{4}$$

Our numerical calculations were performed on the Cray-XMP-48 at the Höchst–Leistungs–Rechen–Zentrum (HLRZ) in Jülich, therefore the vectorization of the computer code was an important aspect. The steps from the spins to the bond-configuration and from the clusters to the spins, as well as the measurement subroutines, are well vectorizable, but contain only very few floating-point operations (mainly logical operations and memory rearrangements). The search of the clusters on the basis of a given bond-configuration is, however, rather hard to vectorize due to the inherent non-local information residing in the clusters. At the end a full updating cycle, the measurement was about a factor 10 slower than a sweep and a measurement with our Metropolis program. For the search of the clusters we applied an algorithm whose execution time grows only linearly with the number of lattice points. The very small clusters (up to $n_c \leq 3$) were filtered out at the beginning by going through every point (this step can be vectorized). The remaining clusters were found by starting from the next "undone" point and collecting all the other points belonging to this cluster before going to the next cluster. Within a cluster, the points were found "generation by generation", where a generation is defined as the set of points in the cluster with given distance from the starting point. (The "distance" is the minimum number of bonds belonging to the cluster between two points in the cluster.) A logical array was used to mark the lattice sites which were already "done", i.e. already associated to some cluster. The different treatment of very small clusters turned out advantageous also for the measurement of the physical quantities. We also compared this algorithm to the

TABLE 1
The results of the numerical calculation in the 3 points denoted by A, B, C. Here only the statistical errors in last numerals are indicated.

	L	κ	m	χ_2	$-\lambda_4$	$\lambda_6 \times 10^{-4}$	C_m	C_χ
A	12	0.0710	0.49032(9)	27.983(5)	40.5(3)	1.44(12)	2.597(5)	0.997(4)
B	16	0.0724	0.37825(18)	45.86(2)	35.0(9)	0.9(3)	2.575(9)	0.990(6)
C	20	0.0732	0.30665(18)	69.95(4)	32.2(12)	0.6(4)	2.595(12)	0.977(9)

more conventional Hoshen–Kopelman algorithm [13] and obtained similar performances.

The hopping parameter values (κ) for the lattices 12^4, 16^4 and 20^4 were chosen in such a way that the finite-volume effects, determined in ref. [7], are already small, in most cases smaller than the statistical errors. This occurs in the intermediate coupling range (where Monte Carlo calculations are feasible) if the product of the mass m and lattice size L is about $mL \sim 6$. For such large volumes the small finite-size corrections are well given by 1-loop lattice perturbation theory [7]. The number of updating cycles and measurements was 7.6×10^6 on the 12^4, 1.6×10^6 on the 16^4 and 1.0×10^6 on the 20^4 lattice. A collection of some directly measured quantities is given in table 1.

The mass m in table 1 is obtained from a single cosh function going through the value of the time-slice of the zero-momentum 2-point function at largest distance $\frac{1}{2}L$ and half the largest distance $\frac{1}{4}L$. The statistical error of the mass and of every other quantity in table 1 is determined by binning the data in large bins (actually of lengths 2^k, k = integer). In every bin the values of the quantities (which are some functions of expectation values) were determined and the errors were estimated from the standard deviation corresponding to the fluctuation of the values in the bins. For some quantities involving large cancellation (e.g. for λ_6) a minimum bin length of the order of 100 was needed in order to obtain reasonable values. For larger bins the error estimate first increased with the bin length, but at a bin length of about 10000 the errors became constant. Note that this way of estimating the errors takes into account the correlation between different expectation values entering the definition of a given quantity. For instance, the time-slices of the 2-point function at distances $\frac{1}{2}L$ and $\frac{1}{4}L$ are highly correlated, therefore there is no simple way to determine the error of the mass from the errors of the 2-point function. In the case of the mass, however, the error in table 1 is not much different from that which is obtained by fitting the 2-point function with a single cosh function and by assuming the independence of the errors at different distances. Of course, in the case of fits the errors depend also on the length of the interval chosen for the fit. The value of the mass obtained from the fits is equal, within 1σ, to the value in table 1. The result of the fits shows that the 2-point function is

strongly dominated by the 1-particle state. Some small higher mass contributions can only be seen at distances less than 3. The constant multiplying the cosh function corresponding to the 1-particle state in the 2-point function is, respectively (in the same order as in table 1): $c = 3.9035(7) \times 10^{-3}$; $c = 2.093(2) \times 10^{-3}$; $c = 1.3330(5) \times 10^{-3}$.

The definition of the other quantities in table 1 is as follows: χ_2 is the susceptibility defined in eq. (2) and $\lambda_{4,6}$ is obtained from the generalized susceptibilities as

$$\lambda_n \equiv m^{2n-4} \frac{\chi_n}{(\chi_2)^{n/2}} . \tag{5}$$

The constants $C_{m,\chi}$ characterize the critical behaviour of the mass and the susceptibility, respectively [2]

$$C_m \equiv \frac{m}{\sqrt{\tau}} |\ln \tau|^{1/6} , \qquad C_\chi \equiv \tau \chi_2 |\ln \tau|^{-1/3} , \tag{6}$$

where $\tau \equiv 1 - \kappa/\kappa_{cr}$. In table 1 the value of the critical hopping parameter was assumed to be $\kappa_{cr} = 0.074834(15)$ [14], and its error was taken into account in the error of $C_{m,\chi}$. As it can be seen from the table, C_m and C_χ are the same within errors in the three points (the deviations are about 2σ). Therefore, the scaling of the mass and susceptibility is well satisfied, including logarithmic corrections to the mean-field critical exponents. The change of the logarithmic factors is an order of magnitude larger than the errors, therefore our data establish the presence of the logarithmic corrections beyond any doubt. The analogous scaling relation for λ_4 is not satisfied, however: it would imply

$$\lambda_4 = -\frac{32\pi^2}{3|\ln \tau|} . \tag{7}$$

As one can see from table 1, the measured values in all the three points are about a factor of 1.15 larger. Since λ_4 is closely related to the renormalized coupling g_R, we shall return to this question below.

In order to compare the results with the analytic calculations one has to introduce the renormalized quantities at zero momenta. The required relations were included in ref. [7], we only repeat them here for convenience of the reader. The connection between the renormalized mass m_R and the physical mass m in 2-loop perturbation theory is given by

$$m = 2 \log \left[\left(1 + \tfrac{1}{4} m_R^2\right)^{1/2} + \tfrac{1}{2} m_R \right] \left(1 - 0.0013 \alpha_R^2\right) , \tag{8}$$

TABLE 2
Comparison of the renormalized quantities to the theoretical predictions in the points A, B, C. Here the errors include also an estimate of the systematic uncertainties.

	m_R	κ^{LW}	Z_R	Z_R^{LW}	g_R	g_R^{LW}	$h_R \times 10^{-4}$	$h_R^{PT} \times 10^{-4}$
A	0.4951(2)	0.0709(2)	0.9746(4)	0.973(9)	42.5(5)	42(7)	1.61(15)	1.74(3)
B	0.3804(3)	0.0724(2)	0.9614(7)	0.973(9)	36.1(11)	33(4)	0.9(3)	1.23(7)
C	0.3078(3)	0.0732(3)	0.9707(8)	0.975(9)	32.9(13)	29(3)	0.6(4)	1.02(8)

where $\alpha_R \equiv g_R/(16\pi^2)$. The ratio $r \equiv m_R/m$ occurs also in the other quantities

$$Z_R = 2\kappa r^2 m^2 \chi_2 , \qquad g_R = -r^4 \lambda_4 , \qquad h_R = r^8 \lambda_6 . \tag{9}$$

Here Z_R is the field renormalization factor, g_R the renormalized coupling and h_R the zero-momentum connected 6-point function. Later on, the modified Z-factor $Z'_R \equiv Z_R/(2\kappa)$ will also be considered. (Note that compared with ref. [3] the notations for Z_R and Z'_R are interchanged here.) The numerical results for the renormalized quantities are compared to the theoretical expectations in table 2. The entries in the table with suffix LW are the results of the analytical calculation of Lüscher and Weisz [3] based on 10th-order hopping parameter expansion and 3-loop perturbative renormalization group equations. The analytical predictions were determined by matching the renormalized mass m_R to the measured value. From the point of view of the renormalization group equations this is the most natural way. In this case the value of the hopping parameter is an output (third column in table 2). The agreement between the numerical data and the analytical calculations is excellent. The numerical errors are usually smaller, nevertheless our errors are understood in the sense of standard deviations, whereas those in ref. [3] are estimates of mathematical bounds on "corridors", which should contain the true results with large probability. In the case of m_R and g_R the numerical results in table 2 include an extrapolation to infinite volume from the measured value at $mL \simeq 6$, using leading-order lattice perturbation theory [7]. These are small corrections but they involve some theoretical uncertainty, therefore 10% of the correction was added to the error as a rough estimate of the systematic error.

The last entry in table 2 is the prediction of 2-loop renormalized perturbation theory for the zero-momentum connected 6-point function

$$h_R = 10 g_R^2 \left(1 - \tfrac{3}{4}\alpha_R + \tfrac{9}{4}\alpha_R^2\right). \tag{10}$$

As table 2 shows, this agrees with the measured numbers within errors. Unfortunately, the statistical errors on the 16^4 and 20^4 lattices are too large. The numerical result on the 12^4 lattice is, however, a non-trivial test of renormalized

perturbation theory in a point where the renormalized coupling is already not very small: the 1-loop correction in eq. (10) is -20% and the 2-loop is $+16\%$.

An important question in the Monte Carlo calculations is the scaling behaviour of the renormalized quantities as a function of the renormalized mass. The renormalized coupling and the field renormalization factor Z'_R satisfy the differential equations [2]

$$m_R \frac{\partial g_R}{\partial m_R} = \beta(g_R, m_R), \qquad m_R \frac{\partial \ln Z'_R}{\partial m_R} = 2\gamma(g_R, m_R). \tag{11}$$

The Callan–Symanzik functions β and γ are given up to 3-loop in the appendix of ref. [3], including the mass-dependence ("a^2-corrections") up to 1-loop. The numerical solution of the equation for g_R with this β-function is shown in fig. 1, starting both at the 12^4 and 16^4 points. As one can see from the figure, the points at smaller mass have a tendency to be at larger couplings, but the deviation is only at the 2σ level, and therefore statistically insignificant. Comparing this 3-loop β-function to the universal 2-loop β-function shows (see fig. 2) that the two points at smaller masses are just in the middle between the 2-loop and 3-loop curves. Therefore, the true β-function is probably somewhere in between, which is rather reasonable since the perturbation series is alternating. Fig. 2 shows that the numerical results on g_R

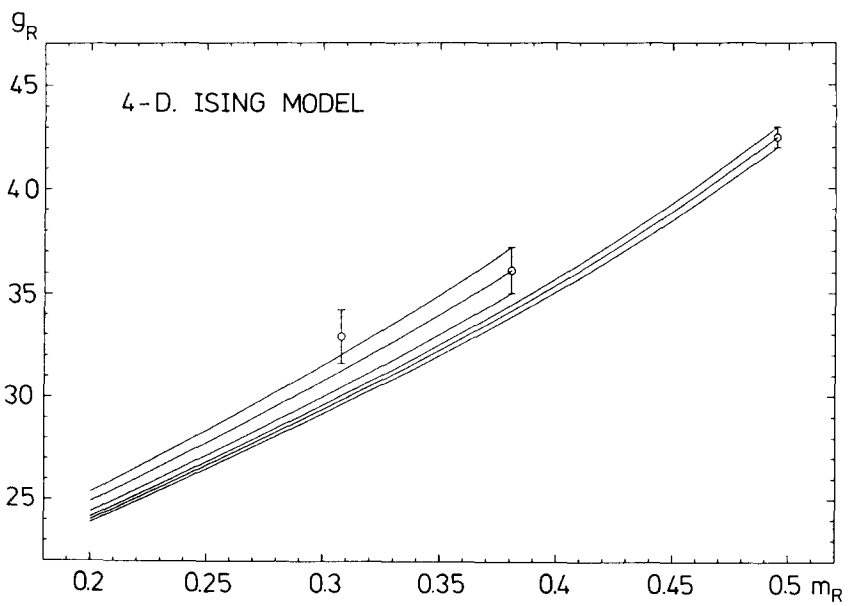

Fig. 1. The result of the numerical integration of the renormalization group equations for the renormalized coupling. The differential equation is started both from the 12^4 and from the 16^4 points.

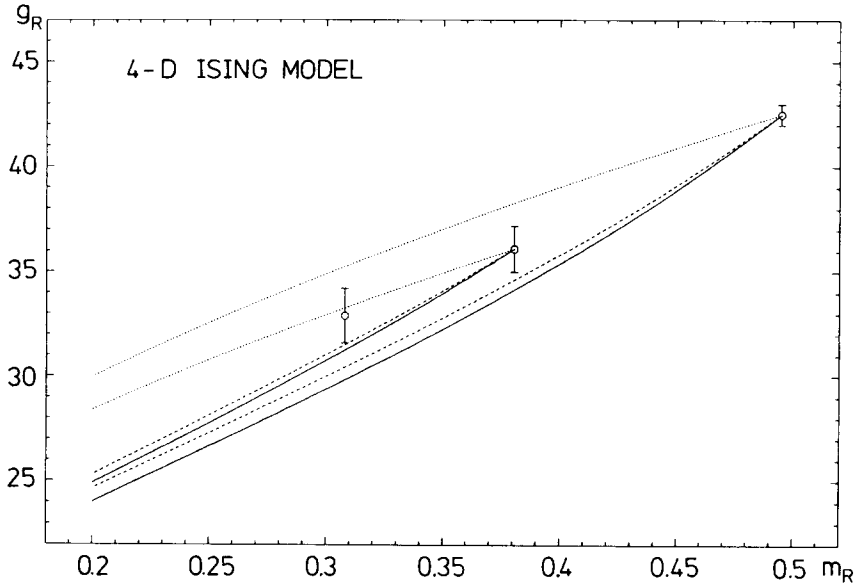

Fig. 2. Comparison of the different approximations to the β-function: full line is 3-loop with a^2-corrections taken into account up to 1-loop, the dashed line is 3-loop without a^2-corrections and the dotted line is 2-loop without a^2-corrections. The numerical integration of the renormalization group equation is started both from the 12^4 and from the 16^4 points.

are statistically consistent also with the universal 2-loop β-function, therefore the deviations from the scaling law (7) could partly be due to a^2-effects. The importance of the a^2-effects can also be seen by numerically integrating the equation for Z'_R in eq. (11). At the level of our small errors, the change of Z'_R is reproduced only qualitatively by the 3-loop γ-function with 1-loop a^2-corrections. But in this case the change is completely dominated by the a^2-effects. Since the constancy of C_χ in table 1 is well satisfied, one can conclude that the scaling violations in Z'_R are probably due to the a^2-effects and not to higher loop corrections. The a^2-corrections are, however, only qualitatively reproduced by the perturbative contributions up to 1-loop.

The measured values at the 20^4 point, which is closest to the critical point, can also be used to start the integration of the renormalization group equations in order to obtain the continuation of the solution in the phase with spontaneously broken symmetry on the other side of the critical point. We applied the same procedure as in ref. [3], taking our more precise data. With the 3-loop Callan–Symanzik functions and the 1-loop a^2-corrections one obtains at the mass $m_R = 0.3$ in the broken phase, $g_R = 26.8 \pm 1.9$ and $Z'_R = 6.10 \pm 0.03$. The error here is only statistical. Taking, as another extreme, everywhere the 2-loop functions without a^2-corrections, the result is $g_R \simeq 30$ and $Z'_R \simeq 6.2$. This shows that the extrapolation is quite sensitive to the

higher corrections in the Callan–Symanzik functions, but the 3-loop result has, of course, a better chance to be correct. A direct numerical check in the broken phase would, however, be quite useful [12].

Finally, let us discuss our experience with the percolation cluster algorithm. As already mentioned before, the updating and measurement is about a factor of 10 slower on our lattices with the cluster algorithm than with the Metropolis algorithm. This is, however, by far compensated by the decrease of the autocorrelation and by less fluctuations of the measured quantities in the cluster representation. In order to quantify the efficiency of the algorithms, we compared the relative errors of a few quantities achieved after the same number of sweeps. For the Metropolis algorithm we took the data on 12^4 and 24^4 from ref. [7] corresponding to a correlation length of about 2 and 5, respectively. For the cluster algorithm, besides the above 12^4 data, we did a shorter 24^4 run at the same hopping parameter as in ref. [7] ($\kappa = 0.074$). In the percolation cluster runs the quantities were determined both in the spin and in the cluster representation, in order to compare the relative errors obtained in both ways. On the 12^4 lattice in the spin representation with the cluster algorithm the errors are by a factor of 2.0 to 2.5 smaller than with the Metropolis algorithm, which implies a reduction of the autocorrelation time by about 5. For χ_2, λ_4, λ_6 and the 2-point function time-slice at largest distance the ratio of errors is multiplied, respectively, by 3, 6, 10 and 4 due to the smaller fluctuations in the cluster representation. Therefore, the total gain in computational speed for these quantities is between 5 and 50. This looks even better on the 24^4 lattice, where the fluctuations are damped by roughly the same factor, but the gain in the error due to shorter autocorrelations is by a factor of 2 larger. This gives a further factor of 4 gain in speed. Therefore, the effect of using the percolation cluster algorithm is rather positive. It would be important to develop similar algorithms also for other lattice models. (For recent attempts see ref. [8] and the related approach in ref. [15].)

In summary the highly efficient percolation cluster algorithm makes it possible to perform a non-trivial test of renormalized perturbation theory and of perturbative scaling. The numerical results are in good agreement with theoretical expectations.

It is a pleasure to thank Martin Lüscher for his interest and help at every stage of this work. U.W. would like to thank the DESY theory group for their hospitality. The calculations presented here were performed on the CRAY X-MP/48 at HLRZ, KFA Jülich.

References

[1] K.G. Wilson, Phys. Rev. B4 (1971) 3184;
K.G. Wilson and J. Kogut, Phys. Rep. 12C (1974) 75;
R. Schrader, Phys. Rev. B14 (1976) 172;
M. Aizenmann, Phys. Rev. Lett. 47 (1981) 1; Commun. Math. Phys. 86 (1982) 1;
J. Fröhlich, Nucl. Phys. B200 [FS4] (1982) 281;

C. Aragao de Carvalho, C.S. Caracciolo and J. Fröhlich, Nucl. Phys. B215 [FS7] (1983) 209;
J. Fröhlich, *in* Progress in gauge field theory, Cargese lecture 1983, ed. G. 't Hooft et al., Plenum Press, New York, 1984) and references therein
[2] E. Brezin, J.C. Le Guillou and J. Zinn-Justin, *in* Phase transitions and critical phenomena, vol. 6, eds. C. Domb, M.S. Green (Academic Press, London, 1976) p. 125
[3] M. Lüscher and P. Weisz, Nucl. Phys. B290 [FS20] (1987) 25; B295 [FS21] (1988) 65
[4] M. Lüscher, lecture given at the NATO Advanced Study Institute on non-perturbative quantum field theory, Cargèse, 1987; DESY preprint 87-159 (1987)
[5] R.H. Swendsen and J.-S. Wang, Phys. Rev. Lett. 58 (1987) 86
[6] P.W. Kasteleyn and C.M. Fortuin, J. Phys. Soc. Jpn. Suppl. 26s (1969) 11;
C.M. Fortuin and P.W. Kasteleyn, Physica 57 (1972) 536
[7] I. Montvay and P. Weisz, Nucl. Phys. B290 [FS20] (1987) 327
[8] U. Wolff, Phys. Rev. Lett. 60 (1988) 1461; DESY preprint 87-092 (1987)
[9] G. Parisi, R. Petronzio and F. Rapuano, Phys. Lett. B128 (1983) 418
[10] R.H. Swendsen, Phys. Rev. Lett. 52 (1984) 1165
[11] N. Metropolis, A.W. Rosenbluth, A.M. Teller and E. Teller, J. Chem. Phys. 21 (1953) 1087
[12] K. Jansen, J. Jersák, I. Montvay, G. Münster, T. Trappenberg, and U. Wolff, work in progress.
[13] J. Hoshen and R. Kopelman, Phys. Rev. B14 (1976) 3438
[14] D.S. Gaunt, M.F. Sykes and S. McKenzie, J. Phys. A12 (1979) 871
[15] G. Mack and K. Pinn, Phys. Lett. B173 (1986) 1434